Case Studies in Construction Materials 16 (2022) e00848

Contents lists available at ScienceDirect

Case Studies in Construction Materials

journal homepage: www.elsevier.com/locate/cscm

Case study

Fatigue effects of embedding electric vehicles Charging Units into electrified road

Claudia Nodari *, Maurizio Crispino, Emanuele Toraldo

Department of Civil and Environmental Engineering, Politecnico di Milano, Piazza Leonardo da Vinci 32, Milan 20133, Italy

ARTICLE INFO

Keywords:
Electrified road
Dynamic charging
Charging Unit (CU)
Finite Element Modelling (FEM)
Fatigue analysis

ABSTRACT

A charging infrastructure network for Battery Electric Vehicles (BEV) is more than an option for the transportation scenarios of the next years. From a pavement engineering point of view, this network consists in prefabricated Charging Units (CU) embedded into the road pavement, generating additional questions related to the structural life of the pavements in which the CU are located. Moreover, even if in the available literature few studies describe the structural response of e-road, the long-term performances of pavements are not fully investigated. This is the reason why this research analyzes fatigue behavior of electrified road (*e-road*) in comparison with traditional road (*t-road*). In particular, the study is devoted to identifying the number of critical load cycles leading to failure an *e-road* pavement. As a second stage, the theoretical and numerical results are verified applying the findings obtained during the first stage of the research to a real case study: Viale Forlanini in Milan (Italy), which is an important two carriageway road connecting the city center to the Linate airport. As a result of these analyzes, interesting outcomes were obtained regarding the fatigue effects of embedding CU into road pavement, estimating the service life and demonstrating that CU seems to be compatible with the structural effectiveness of the pavement, as also confirmed by the case study results.

1. Introduction

A potential solution to improving the environmental sustainability of the transportation systems over the incoming years is the use of Battery Electric Vehicles (BEV), that are entirely powered by batteries. In order to charge BEV, on-the-road (dynamic) charging appears to be a promising solution, that overcomes long waiting time and range anxiety [1]. This on-the-road charging system requires a new charging infrastructure network. In other words, a change of roads paradigm is needed, therefore traditional roads (*t-roads*) have to switch into electrified roads (*e-roads*). Regarding the charging systems, which are not the focus of this paper, the available literature suggests that the Wireless Power Transmission systems (such as Inductive Power Transfer) are contactless charging technologies, that deliver electrical energy to BEV at a gap distance [1]. From a road point of view, it implies that prefabricated Charging Units (CUs) must be embedded into the road pavements with the goal of creating the aforementioned on-the-road charging system. Each CU is a cement concrete box, in which the electric technologies are allocated, opened on the two sides close to the other CU [1].

In the available literature few studies describe the structural response of *e-road*, without considering long-term performances of pavements. Therefore, based on previous research of the authors [1], the objective of this investigation is to analyze fatigue behavior of *e-road* in comparison with *t-road*. Using a Finite Element Model (FEM), stresses and strains are determined for different cross-sectional

* Corresponding author.
E-mail addresses: claudia.nodari@polimi.it (C. Nodari), maurizio.crispino@polimi.it (M. Crispino), emanuele.toraldo@polimi.it (E. Toraldo).

https://doi.org/10.1016/j.cscm.2021.e00848
Received 28 September 2021; Received in revised form 29 November 2021; Accepted 19 December 2021
Available online 20 December 2021

geometries: *t-road*, *e-road_solid CU* (CU as a solid box, according to the way in which it is simulated by the available literature [2]) and *e-road_void CU* (having a void for allocating the electric technologies).

2. Literature review

Fatigue cracking is a structural distress that leads to a reduction in the serviceability of asphalt pavement, resulting from the repeated application of traffic loads lower than the tensile strength of the materials [3].

Fatigue cracking simulation is based on the cumulative damage concept given by Miner's approach [4]. The incremental Damage Index (*DI*) is calculated as the ratio of the actual number of traffic repetitions to the allowable number of axle loads -Eq. (1)-. Ideally, fatigue cracking should occur at *DI* equal to 1 [4].

$$DI = \sum_{i=1}^{T} \frac{n_i}{N_{fi}} \tag{1}$$

Where:

DI = Damage Index;

T = total number of periods;

n_i = actual number of traffic repetitions in period i;

N_{fi} = allowable number of axle loads (that leads to failure) in period i.

The most used model to calculate the allowable number of axle loads N_f is a function of the tensile strain and mix stiffness, as the one developed by the Asphalt Institute -Eq. (2)- [4].

$$N_f = 0.00432 \quad \bullet C \bullet \left(\frac{1}{\varepsilon_t}\right)^{3.291} \left(\frac{1}{E}\right)^{0.854} C = 10^M M = 4.84 \bullet \left(\frac{V_b}{V_a + V_b} - 0.69\right) \tag{2}$$

Where:

C = laboratory to field adjustment factor;

V_b = effective binder content by volume(%);

V_a = air voids in the HMA mixture(%);

ε_t = horizontal tensile strain at the critical location;

E = stiffness of Hot Mix Asphalt (HMA) measured in [psi];

0.00432, 3.291 and 0.854 = laboratory regression coefficient.

The Asphalt Institute 9th Edition of the Design Manual introduced a field calibration factor for adjusting the laboratory results to the field responses -Eq. (3)- [4]. In the following, this model will be the *Standard Model*.

$$N_f = 0.00432 \quad \bullet 18.4 \bullet C \bullet \left(\frac{1}{\varepsilon_t}\right)^{3.291} \left(\frac{1}{E}\right)^{0.854} \tag{3}$$

Historically, fatigue cracking is considered to initiate at the bottom of the asphalt layer due to excessive tensile stresses/strains, and then to propagate upwards to the surface (bottom-up or alligator cracking). However, many laboratory investigations and *in-situ* studies have shown that fatigue cracking can also start at the surface of the pavements and then propagate downwards through the asphalt layer (top-down or longitudinal cracking) [3,5]. Therefore, both cases may exist, depending on the location of the maximum horizontal tensile strains in the asphalt layer. Several factors influence the tensile stress-strain fatigue behavior of pavements affecting the mechanism of crack initiation, such as tire-pavement contact pressure, pavement structure and layers mechanical characteristics [5]. In particular, some studies detect the critical location of top-down cracking near or within the tire-pavement contact area [5,6].

Therefore, a new formulation of the model to calculate N_f -Eq. (4)- was proposed by AASHTO in MEPDG [7] to predict both types of load related cracks: bottom-up and top-down cracking.

$$N_f = 0.007566 \quad \bullet C \bullet C_H \bullet \left(\frac{1}{\varepsilon_t}\right)^{3.9492} \left(\frac{1}{E}\right)^{1.281} \tag{4}$$

Where:

C_H = thickness correction term, dependent on type of cracking.

For bottom-up cracking -Eq. (5)-:

$$C_H = \frac{1}{0.000398 + \frac{0.003602}{1+e^{11.02-3.49 \bullet H_{HMA}}}} \tag{5}$$

For top-down cracking -Eq. (6)-:

$$C_H = \frac{1}{0.01 + \frac{12}{1+e^{15.676-2.8186 \bullet H_{HMA}}}} \tag{6}$$

Where:

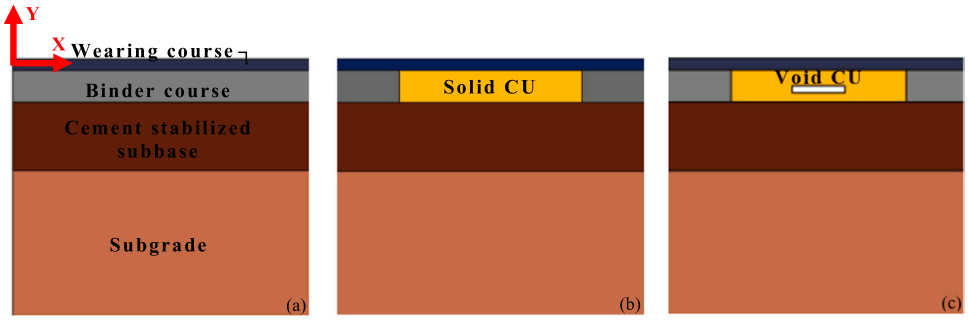

Fig. 1. Cross-sectional geometry (a) t-road (b) e-road_solid CU (c) e-road_void CU [1].

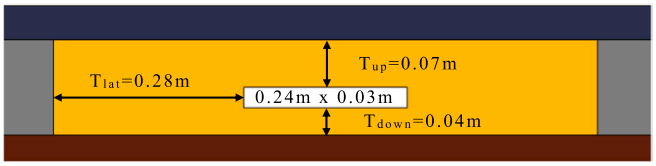

Fig. 2. Void CU details [1].

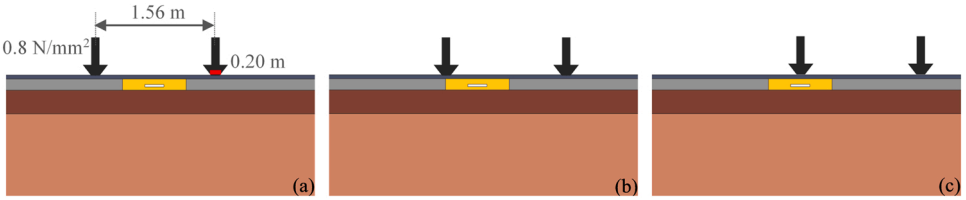

Fig. 3. Load positions (a) centered on CU (b) CU edge (c) CU center [1].

Table 1
Layers and key material main characteristics [1].

	Wearing Course	Binder Course	Cement stabilized subbase	Subgrade	Concrete CU
Thickness [m]	0.05	0.14	0.30	6.00	0.14
Bulk density [N/m^3]	24,000	23,500	23,000	21,000	23,000
Young's modulus [N/mm^2]	5500	3500	2000	800	25,000
Poisson's Ratio [-]	0.35	0.35	0.20	0.30	0.20

H_{HMA} = total HMA thickness in [in].

3. Objectives

The present study is divided in two stages. The goal of the first one is to describe fatigue cracking from a general point of view. Therefore, different cross-sectional geometries (*t-road* and *e-road*) are analyzed using three fatigue cracking models (standard, bottom-up and top-down). In detail, the objectives of this first stage are: (i) the identification of the appropriate model, also verified by its application on a real case-study (the second part of this research); (ii) the calculation of the number of the critical load cycles leading to failure; (iii) the evaluation of CU effect on the pavement performances.

Based on these results, the second phase is devoted to validate the achievements of the first one by applying them to a real case study carried out on Viale Forlanini in Milan (Italy), which is an important two carriageway road, connecting the city center to the Linate airport. Therefore, the cross-sectional geometries are analyzed using real traffic loads and bituminous mixtures for wearing/binder courses (previous studied in [8,9]). The actual traffic is compared with the critical load cycles of the first phase to evaluate the long-term effects of CU into pavement as regard long-term (fatigue) performances.

Table 2
Young's modulus of asphalt layers at different seasons.

		Young's modulus [N/mm^2]		
		E (spring/autumn)	E + 50% (winter)	E-50% (summer)
Asphalt layers	Wearing course	5,500	8,250	2,750
	Binder course	3,500	5,250	1,750

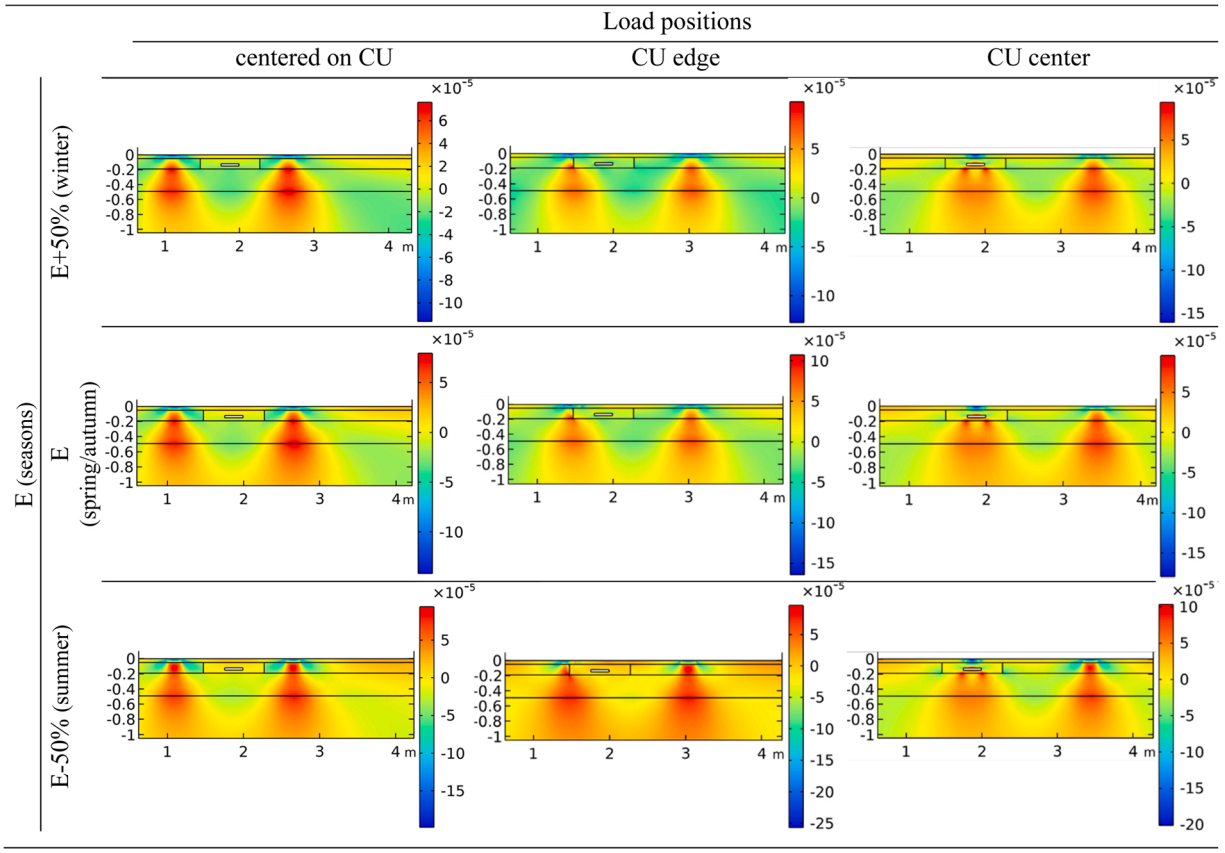

Fig. 4. Distribution of horizontal strains ε_{xx} of e-road_void CU at different seasons and different load positions.

4. General assessment of fatigue cracking

4.1. Methodology

Three cross-sectional geometries are analyzed, as indicated in Fig. 1: *t-road, e-road_solid CU and e-road_void CU*, whose cavity dimension is shown in Fig. 2. Moreover, different load positions are considered to explain cross wander distance compared to CU (0.80 m in width and 0.14 m in height) location, as presented in Fig. 3. Table 1 summarized the main characteristics of each layer, in terms of thickness and material properties. More details regarding geometry and materials, wheel pressure (0.8 N/mm^2) and boundary conditions are given in [1].

Since the characteristics of each layer are based on typical materials properties [1], to evaluate the asphalt layers behavior at low (winter) and high (summer) temperatures, Young's modulus at 20 °C was increased and decreased by 50% respectively, as reported in Table 2.

Based on these conditions, 9 simulations are carried out using a Finite Element Model (FEM) software -COMSOL Multiphysics 5.5- to calculate stresses and strains throughout the domain at each temperature (total of 27 simulations). Complete adherence between superimposed layers was assumed.

As regard long-term performances of pavements, fatigue cracking prediction is based on Miner's law -Eq. (1)-, that is made clear in Eq. (7) considering the behavior in each season of the year.

Table 3
Depth of $\varepsilon_{xx,\ max}$ @E-50% (summer).

Depth of $\varepsilon_{xx,\ max}$ [m]		Load positions		
		centered on CU	CU edge	CU center
cross-sectional geometries	*t-road*	-0.116	-0.104	-0.117
	e-road_solid CU	-0.109	-0.113	-0.106
	e-road_void CU	-0.109	-0.19 (CU)	-0.12 (CU)

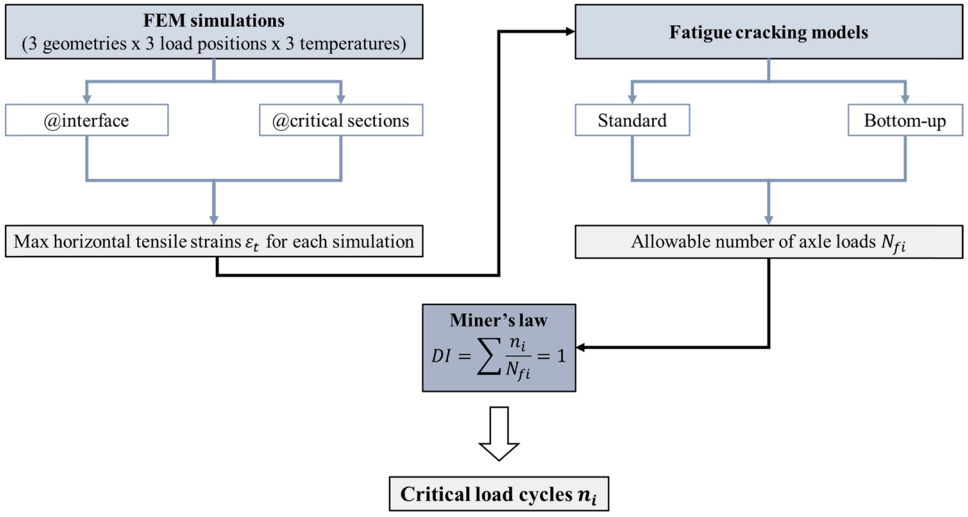

Fig. 5. Experimental plan flow diagram of the general part.

$$DI = \sum_i \frac{n_i \bullet m_i}{N_{f,i}} = \frac{n_w \bullet m_w}{N_{f,winter}} + \frac{n_s \bullet m_s}{N_{f,summer}} + \frac{n_{sp/a} \bullet m_{sp/a}}{N_{f,spring/autumn}} = \frac{\frac{n}{12} \bullet m_w}{N_{f,winter}} + \frac{\frac{n}{12} \bullet m_s}{N_{f,summer}} + \frac{\frac{n}{12} \bullet m_{sp/a}}{N_{f,spring/autumn}} \tag{7}$$

Where:

DI = Damage Index;
n_i= actual number of traffic repetitions in each season;
m_i = number of months in each season;
$N_{f,i}$ = allowable number of axle loads (that leads to failure) in each season, calculated with the three models;
m_w = number of months in winter in one year, equal to 3;
m_s = number of months in summer in one year, equal to 3;
$m_{sp/a}$ = number of months in spring and autumn in one year, equal to 6;
n = actual number of traffic repetitions, equally distributed in each season;
12 = number of months in one year.

As reported in Section 2, theoretically, fatigue cracking should occur at *DI* equal to 1. Therefore, the objective is the calculation of the actual number of traffic repetitions n that leads to that damage value -Eq. (8)-.

$$n = \frac{12 \bullet N_{f,winter} \bullet N_{f,summer} \bullet N_{f,spring/autumn}}{m_w \bullet N_{f,summer} \bullet N_{f,spring/autumn} + m_s \bullet N_{f,winter} \bullet N_{f,spring/autumn} + m_{sp/a} \bullet N_{f,winter} \bullet N_{f,summer}} \tag{8}$$

The allowable number of axle loads $N_{f,i}$ is calculated using the three models (standard, bottom-up and top-down) described in Section 2. Recalling the expressions of the formulas of $N_{f,i}$ (Eq. (3) - Eq. (6)) the following data are used:

- ε_t: horizontal tensile strains obtained as outputs of the FEM simulations, depending on cross sectional geometries, load positions and seasons (an example is given in Fig. 4);
- E: stiffness of the HMA depending on seasons (as described in Table 2);
- V_b: effective binder content equal to 5% (in the recommended range of the Italian Specification for asphalt layer [10]);
- V_a: air voids content equal to 4% (higher than the inferior limit defined in the Italian Specification for asphalt layer [10]);
- H_{HMA}: total HMA thickness equal to 0.19 m (0.05 m of wearing course and 0.14 m of binder course [1]).

A representative case of strains is shown in Fig. 4, in which horizontal strains ε_{xx} of *e-road_void CU* are presented for different

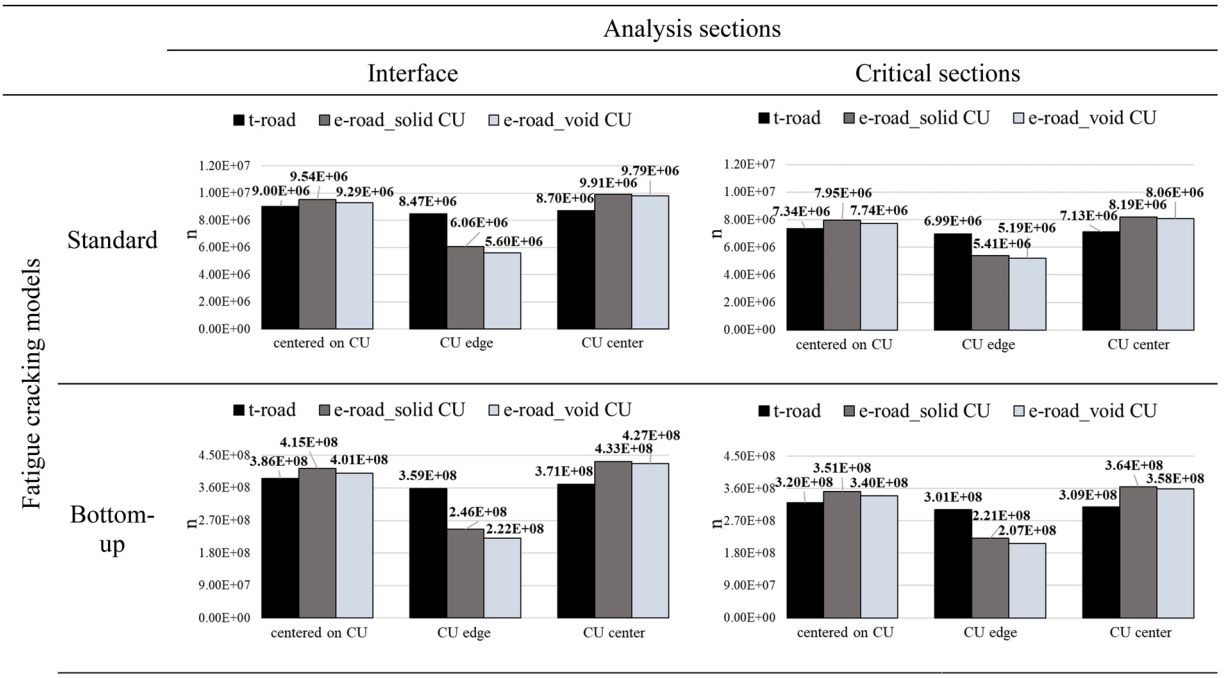

Fig. 6. Number of traffic repetitions n corresponding to DI = 1.

seasons according to the three load positions previously detailed. The FEM results reveal that the horizontal strains ε_{xx} is close to the applied load. Strain distribution changes when load is on CU edge or on CU center due to the presence of the concrete CU.

Considering asphalt layers strains of all the cross-sectional geometries and load positions (that for the sake of simplicity are omitted), it is possible to note that maximum values of ε_{xx} are along *binder course – cement stabilized subbase* interface at intermediate and low temperatures (E and E + 50% respectively). Instead, at high temperature (E-50%), maximum horizontal strains values are concentrated at different depths, as reported in Table 3. The mean value is equal to − 0.11 m, approximately in the middle of the binder layer.

To take into account what before described, N_f is, therefore, calculated along two sections: interface and critical sections. In the first condition, strains are computed along *binder course – cement stabilized subbase* interface for each temperature. Instead, in the case of critical sections, strains are determined: along interface for both intermediate and low temperatures; along section at −0.11 m for high temperature.

The experimental plan of the first part of the research is summarized in Fig. 5.

4.2. Results and discussion

The results obtained from the use of Miner's law are presented in Fig. 6, in which the number of traffic repetitions corresponding to $DI = 1$ is shown for both standard and bottom-up models according to different analysis sections. In each graph, the results are also divided according to load positions and cross-sectional geometries.

The outcomes achieved using top-down models are not disclosed for the reasons listed below:

- Even if top-down cracks may occur earlier, they do not significantly reduce the structural integrity of the asphalt layer [3]. Therefore, bottom-up fractures are considered as more critical than the top-down ones.
- As shown in Fig. 4, the maximum tensile horizontal strains do not appear along the surface of pavement (condition suggested by [5, 6]). Therefore, top-down cracks seem to be less probable than bottom-up phenomenon.
- Based on the study discussed in [3], in cement stabilized base pavement (like the one considered in the present research) cracks develop initially at the bottom of asphalt layer. Therefore, again, top-down cracks seem to be less probable than bottom-up phenomenon.

Despite both the fatigue cracking models and the analysis sections, all the graphs are characterized by the same trend of load cycles number. For example, when load is on CU edge, the traffic repetitions of *t-road* are always higher than the ones of *e-roads*; opposite behavior is evident when loads are centered on CU or in CU center.

Regardless of the models, when load is centered on CU and in CU center it is possible to note an increase of the number of traffic repetitions of *e-roads* compared to *t-road*, that means an improvement in fatigue life. In particular, the number of load cycles grows

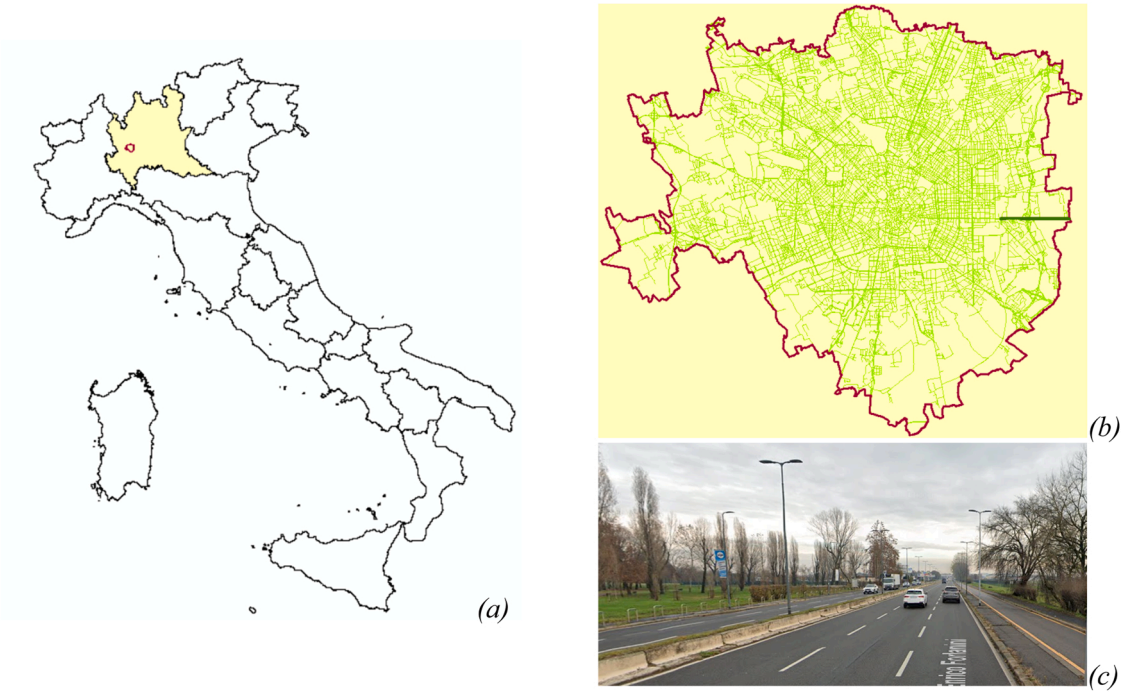

Fig. 7. (a) Location of Milan into Italy; (b) location of Forlanini Avenue into Milan; (c) detail of Forlanini Avenue [12].

Table 4
Mean temperatures of both air and pavements for each season.

		T_{air} [°C]	$T_{pavement}$ [°C]
Seasons	Winter	4	8
	Spring/Autumn	15	21
	Summer	24	34

from 6% to 18% in the case of *e-road_solid CU* and from 3% to 16% for *e-road_void CU* compared to the traditional pavement. Therefore, the CU has a stiffening positive effect on the cross-sectional geometries. On the contrary, when load is on CU edge, the number of traffic repetitions decreases of 27% and of 32% compared to *t-road*, respectively for *e-road_solid CU* and *e-road_void CU*. Therefore, this load position appears as the most critical. This behavior can be explained using results of Fig. 4, in which the strain distributions in binder layer are strongly affected by the presence of the CU.

As regard analysis sections, the evaluation of the strains at the critical sections reveals that the number of traffic repetitions is lower than the one calculated at the interface. Therefore, the critical section approach is more precautionary in terms of fatigue life. However, the critical sections results grow from 6.37% to 18.49% compared to the ones at the interface. Consequently, due to these small differences, it is possible to calculate strains only at the interface. The latter approach is faster than the determination of the sections in which strain values are the highest.

Concerning the comparison between the two fatigue cracking models, bottom-up results are 42 times higher than the ones obtained with standard model. Therefore, the basic approach seems to be more precautionary in terms of fatigue life. However, the formulation of the standard model -Eq. (3)- does not consider the total thickness of asphalt layers. For this reason, the number of traffic repetitions calculated with the bottom-up model is considered as more rigorous and representative of the pavement fatigue life.

Based on these results, the lowest number of load cycles is equal to $2.22 \cdot 10^8$. The value is obtained using bottom-up model, calculating strains at the interface, considering load on CU edge and *e-road_void CU*. This number is used as the highest number of traffic repetitions acceptable on the pavement ($DI = 1$) in the second part of the research concerning real case study.

5. Fatigue assessment of a case study

5.1. Methodologies

As afore mentioned, Viale Forlanini in Milan (Italy) is chosen as case study. It is located in the east part of Milan (Fig. 7). This road, that joins the city of Milan with Linate Airport, is a dual two/three-lane carriageway.

Table 5
Number of traffic repetitions according to load conditions.

		Number of traffic repetitions *n*
Traffic conditions	One lane	$5.75 \cdot 10^7$
	Two lanes	$2.88 \cdot 10^7$

Table 6
Key characteristics of asphalt layers, derived from previous studies ([8,9]).

	Bulk density [N/m^3]	Poisson's Ratio [-]	Young's modulus [N/mm^2] @ 2 Hz		
			@ 8 °C	@ 21 °C	@ 34 °C
Wearing Course	24,240	0.35	17,502	8,092	2,822
Binder Course	23,970	0.35	17,242	8,610	3,363

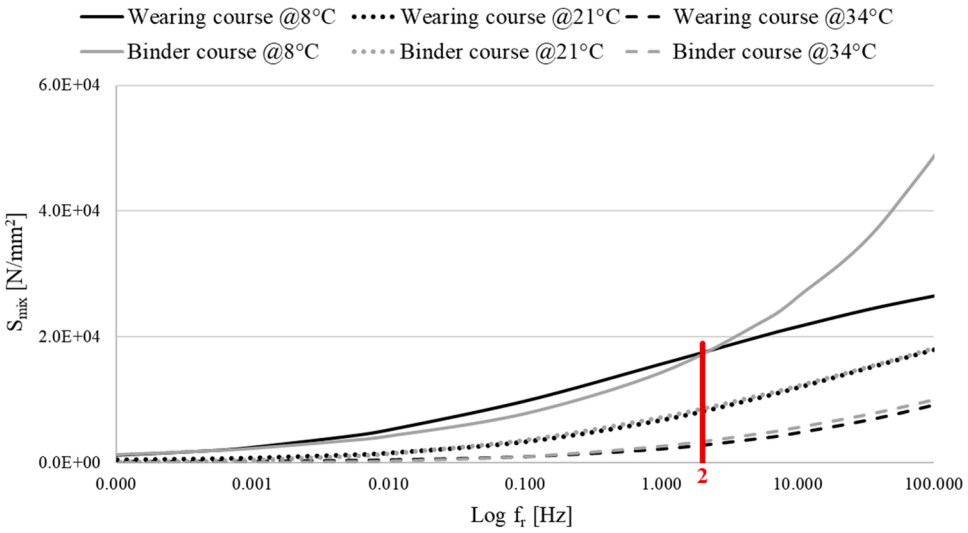

Fig. 8. Master Curves of Wearing Course and Binder Course obtained with AASHTO TP-62 model.

In this part of the research, with the goal of validating the results of the first one, both temperatures and actual traffic repetitions are defined. Based on the data collected on the Linate Airport weather station (very close to Viale Forlanini), monthly mean temperatures of air of the last ten years are calculated. Starting from that, the temperatures into the pavement layers are estimated using an Italian method [11] -Eq. (9)-, obtaining the results reported in Table 4.

$$T_{pav}(z) = (1.467 + 0.043 \cdot z) + (1.362 - 0.005 \cdot z) \cdot T_{air} \quad (9)$$

Where:

$T_{pav}(z)$ = pavement temperature at depth z;

z = pavement depth (measured form surface) at which temperature is calculated;

T_{air} = mean air temperature.

The number of load repetitions during pavement service life (equal to 20 years) is calculated based on the rush hour traffic defined in the Sustainable Urban Mobility Plan of the city of Milan [13] and on the traffic composition of "extra-urban roads characterized by high traffic" [14]. Two load conditions are considered: (i) the vehicles travel on one lane only; (ii) the vehicles travel equally distributed on two lanes. Table 5 shows the number of traffic repetitions used in Miner's law to evaluate the fatigue life of pavements.

Both the cross-sectional geometries and the load positions are the same analyzed in the general part (Fig. 1 - Fig. 3).

Regarding materials, the differences concern the asphalt layers, whose characteristics are reported in Table 6. Young's modulus values are evaluated at the three temperatures of 8 °C (winter), 21 °C (spring/autumn) and 34 °C (summer), according to Table 4. These moduli are obtained using Master Curves approach at a frequency of 2 Hz, based on the stiffness tests results presented in previous studies ([8,9]). Fig. 8 shows Master Curves calculated with AASHTO TP-62 model.

Considering these conditions, 27 FEM simulations are performed to calculate stresses and strains throughout the domain. The quantities of main interest are maximum horizontal tensile strains at *binder course-cement stabilized subbase* interface.

As regard pavements fatigue life, Miner's law is used -Eq. (7)- considering the cumulative damage *DI* as unknown. In this case, *n* is

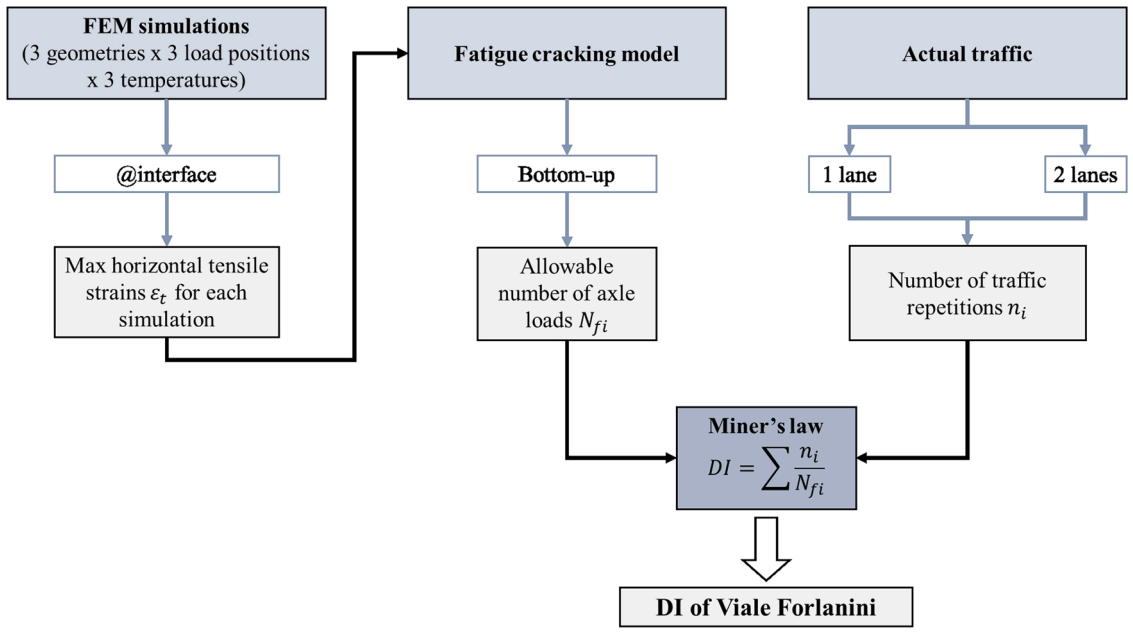

Fig. 9. Experimental plan flow diagram of the case study.

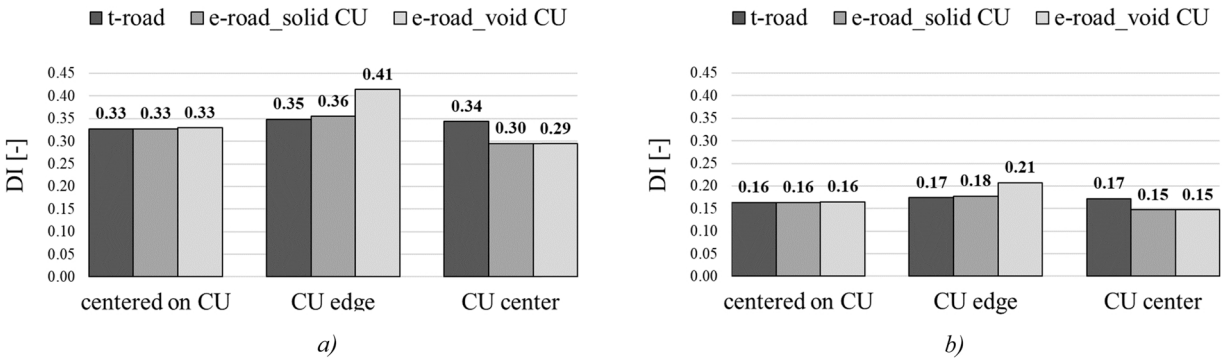

Fig. 10. Damage Index considering a) traffic on one lane; b) traffic on two lanes.

the actual number of traffic repetitions on one lane or on two lanes, according to the previous two load cycles conditions (Table 5). $N_{f,i}$ is the allowable number of axle loads (that leads to failure) in each season calculated with bottom-up model.

Recalling the expressions of the formulas of $N_{f,i}$ (Eq. (3) - Eq. (6)) the following data are used:

- ε_t: maximum horizontal tensile strain along interface obtained as outputs of the FEM simulations. It changes with cross sectional geometries, load positions and seasons;
- E: binder layer stiffness that depends on seasons (as described in Table 6);
- V_b: effective binder content equal to 4.8% (Table 3 in [8]);
- V_a: air voids content equal to 3.85% (Fig. 3 in [8]);
- H_{HMA}: total HMA thickness equal to 0.19 m (0.05 m of wearing course and 0.14 m of binder course [1]).

The experimental plan of the second part of the research herein described is shown in Fig. 9.

5.2. Results and discussion

The results obtained from the applications of the Miner's law are given in Fig. 10, in which the Damage Index is shown for the two traffic conditions according to load positions and cross-sectional geometries.

Comparing the two traffic conditions, it is possible to observe that when vehicles travel on one lane *DI* values are higher (about double) than the results obtained for two lanes. This is predictable because the traffic on one lane is the double of the traffic on two

lanes. Therefore, the greater the traffic, the greater the pavement damage.

Both graphs of Fig. 10 are characterized by the same trend of *DI*. When load is centered on CU, there is no difference in *DI* between the cross-sectional geometry. When load is on CU center, the damage of *e-roads* is lower (about 14%) than the one obtained for *t-road*. This means that CU has a stiffening positive effect on the cross-sectional geometries, according to the results obtained in the general part (4.2). On the contrary, when load is on CU edge, *DI* of *e-roads* is higher (1.96% for *e-road_solid CU* and 19% for *e-road_void CU*) than the one of *t-road*. Once again, this load position appears as the most critical.

Despite the small differences among cross-sectional geometries and load positions, *DI* values are significantly lower than 1 (at which theoretically fatigue cracking should occur) even in case of traffic on one lane (equal to $5.75 \cdot 10^7$). This result is in line with the outcome of the first part, in which the number of traffic repetitions that lead to failure is $2.22 \cdot 10^8$.

6. Conclusions

Dynamic charging of Battery Electric Vehicles (BEV), which seems to be one of the most promising solutions to face of the new challenges of transportation sustainability, requires a proper charging infrastructure network (made of a sequence of Charging Units - CU) embedded into the road pavement. This means that huge investments are needed to convert the traditional roads (*t-roads*) to electrified roads (*e-roads*). These investments have to be supported by engineering solutions for ensuring that the charging infrastructures not negatively affect the road pavement service life. This is the reason why the research described in this paper was devoted to investigating the fatigue behavior of *e-roads*, also in comparison with *t-roads*, as a first stage. The assessment of the first-stage results by applying them to a real case study, was the goal of the second stage of the research.

Regarding the first stage of the research, among the others discussed in the paper, the main finding is that the fatigue performances of *e-roads* are strictly related to the load position. In fact, as shown in Fig. 6, when load is both centered on CU and on CU center, satisfactory fatigue performances are obtained, even better of the results obtained for the traditional pavement. However, in the latter case (load on CU center) battery charging efficiency problems can arise, even if such case appears to guarantee the best fatigue performances. This is the reason why the load position centered on CU seems to be the best solution to combine the pavement fatigue life expectations and the charging needs. Moreover, the results show a decreasing of fatigue performances in case of load on CU edge, even if also in this case the pavement fatigue performances seem to be acceptable.

As regard the case study, the outcomes confirmed the results of the general stage of the research, also considering highly conservative traffic conditions.

It is opinion of the Authors that the results presented in this study can be considered just a step forward on the knowledge about the structural effects of charging networks into *e-road* pavements. Other aspects need to be investigated, such as rutting effects and structural optimization of CU shape from a laboratory and numerical point of view. Moreover, real scale tests are needed for both validating the results herein presented and construction phases optimization purposes.

Declaration of Competing Interest

The authors declare that they have no known competing financial interests or personal relationships that could have appeared to influence the work reported in this paper.

Acknowledgments

The Authors acknowledge Eng. M. Ricci for his contribution in calculations.
The authors report no declarations of interest.
This research did not receive any specific grant from funding agencies in the public, commercial, or not-for-profit sectors.

References

[1] C. Nodari, M. Crispino, M. Pernetti, E. Toraldo, Structural Analysis of Bituminous Road Pavements Embedding Charging Units for electric Vehicles, Springer, 2021, pp. 149–162.
[2] F. Chen, R. Balieu, E. Córdoba, N. Kringos, Towards an understanding of the structural performance of future electrified roads: a finite element simulation study, Int. J. Pavement Eng. 20 (2019) 204–215, https://doi.org/10.1080/10298436.2017.1279487.
[3] Li Yongqi, Asphalt Pavement Fatigue Cracking Modeling, Louisiana State University - LSU Historical Dissertations and Theses, 1999. ⟨https://digitalcommons.lsu.edu/gradschool_disstheses/6999⟩.
[4] NCHRP, Guide for Mechanistic-Empirical Design of New and Rehabilitated Pavement Structures - Appendix II-1, (2004).
[5] X. Hu, L.F. Walubita, Modelling tensile strain response in asphalt pavements: bottom-up and/or top-down fatigue crack initiation, Road Mater. Pavement Des. 10 (2009) 125–154, https://doi.org/10.1080/14680629.2009.9690185.
[6] D. Grellet, G. Doré, J.P. Bilodeau, T. Gauliard, Wide-base single-tire and dual-tire assemblies: comparison based on experimental pavement response and predicted damage, Transp. Res. Rec. 2369 (2013) 47–56, https://doi.org/10.3141/2369-06.
[7] AASHTO, Mechanistic-Empirical Pavement Design Guide - A Manual of Practice, 2015. https://doi.org/10.1201/b17043–14.
[8] C. Nodari, M. Crispino, E. Toraldo, Bituminous mixtures with high environmental compatibility: laboratory investigation on the use of reclaimed asphalt and steel slag aggregates 76 2020 433 442 doi: 10.1007/978-3-030-48679-2_41.
[9] C. Nodari, M. Crispino, E. Toraldo, Laboratory investigation on the use of recycled materials in bituminous mixtures for dense-graded wearing course, Case Stud. Constr. Mater. 15 (2021), e00556, https://doi.org/10.1016/j.cscm.2021.e00556.
[10] ANAS S.p.A:, Capitolato Speciale d'Appalto, Parte 2 Norme Tecniche, Pavimentazioni stradali/autostradali ed. 2010, n.d.
[11] M.C. Marchionna, M.G. Fornaci, M. Malgarini, Modello di Degradazione Strutturale Delle Pavimentazioni, (1985).

[12] Google Maps - Viale Forlanini, (n.d.). ⟨https://www.google.it/maps/@45.4618283,9.2655403,3a,75y,91.92h,83.2t/data=!3m6!1e1!3m4!1sWkb2×09xzOBQ0JBipIXSNQ!2e0!7i16384!8i8192⟩ (accessed May 25, 2021).
[13] Comune di Milano, PUMS - Piano Urbano della Mobilità, (n.d.). https://www.comune.milano.it/aree-tematiche/mobilita/pianificazione-mobilita/piano-urbano-della-mobilita (Accessed 26 May 2021).
[14] Consiglio Nazionale delle Ricerche (CNR), Catalogo delle Pavimentazioni Stradali, Roma (1994).